Original Article

Fibrinogen/poly(L-lactide-co-caprolactone) copolymer scaffold: A potent adhesive material for urethral tissue regeneration in urethral injury treatment

Wei Jiao [a], Wandong Yu [a], Yangyun Wang [a], Jun Zhang [a], Yang Wang [a], Hongbing He [b], Guowei Shi [a, *]

[a] Department of Urology, Shanghai Fifth People's Hospital, Fudan University, No. 801 Heqing Road, Minhang District, Shanghai 200240, China
[b] Shanghai Songli Biotechnology Co., Ltd, Shanghai 201206, China

A B S T R A C T

Since a scarcity of sufficient grafting materials, several complications can arise after urothelial defect reconstruction surgery, including severe hypospadias. Accordingly, developing alternative therapies, such as urethral restoration via tissue engineering are needed. In the present study, we developed a potent adhesive and repairing material using fibrinogen-poly(L-lactide-co-caprolactone) copolymer (Fib-PLCL) nanofiber scaffold to achieve effective urethral tissue regeneration after seeding with epithelial cells on the surface. The in vitro result found the Fib-PLCL scaffold promoted the attachment and viability of epithelial cells on their surface. The increased expression levels of cytokeratin and actin filaments were observed in Fib-PLCL scaffold than PLCL scaffold. The in vivo urethral injury repairing potential of Fib-PLCL scaffold was evaluated using a rabbit urethral replacement model. In this study, a urethral defect was surgically excised and replaced with the Fib-PLCL and PLCL scaffolds or autograft. As expected, the animals healed well after surgery in the Fib-PLCL scaffold group, and no significant strictures were identified. As expected, the cellularized Fib/PLCL grafts have induced the luminal epithelialization, urethral smooth muscle cell remodelling, and capillary development all at the same time. Histological analysis revealed that the urothelial integrity in the Fib-PLCL group had progressed to that of a normal urothelium, with enhanced urethral tissue development. Based on the results, the present study suggests that the prepared fibrinogen—PLCL scaffold is more appropriate for urethral defect reconstruction.

© 2023, The Japanese Society for Regenerative Medicine. Production and hosting by Elsevier B.V. This is an open access article under the CC BY-NC-ND license (http://creativecommons.org/licenses/by-nc-nd/4.0/).

1. Introduction

Since urethral wounds are infrequent, their occurrence has already been growing due to an increase in the number of highway vehicle accidents [50]. The preponderance of urethral injuries can be caused by either blunt trauma to the abdominal (typically coupled with a pelvic fracture) or straddling damage to the pelvis [38]. Urethral injuries caused by a pelvic fracture are frequently accompanied by numerous internal injuries (bladder, spleen, liver, and colon) and a higher risk of death [37,5]. Urethral injuries can also result in incapacitating problems such as urethral constriction, urine dysfunction, and infertility [6]. To minimize these severe sequelae, a fast detection and categorization of the condition, as well as suitable therapeutic plans are necessary [30].

Patients with urethral stricture who have had many operations are no longer being able to have urethral restoration using only donor transplants [26]. Given the significant complexities and constraints of urethral reconstruction, it is critical to create a novel therapeutic strategy, such as a tissue engineering-based strategy with scaffold materials [51]. Tissue engineering technology could potentially being capable of providing non-urological transplants for urethral restoration, resolving the scarcity dilemma of original source material [8,2,27]. Nowadays, tissue engineering has emerged as a viable new treatment option for urological and reproductive problems [28]. Urethral abnormalities are rather frequent and are often caused by trauma, infection, iatrogenic

causes, or congenital illnesses like as hypospadias [6]. There seem to be several types of materials available right now for urothelial tissue reconstruction [39]. *In vitro* cultivation of human urothelium or smooth muscle cells can be used to create autologous cells derived decellularized scaffolds [7]. A possible option for urethral tissue repair is the use of tissue-engineered scaffolds containing autologous cells [41]. Unfortunately, urethral stricture has been one of the fundamental drawbacks of contemporary designed urethral transplants [27]. Since the autologous cells-derived scaffolds have low mechanical strength, they are readily destroyed and hence cannot respond adequately of urethral restoration [23]. Also, it will be tubularized into a tube and anastomosed with the urethra during urethral reconstruction [1]. After the catheter is withdrawn, the urethra fades into obscurity and contracts, culminating in urethral stricture and treatment failure [13]. This restriction is mostly owing to inefficient urethral tissue regeneration and the transition of smooth muscle cells from the contractile to the synthetic phenotype [19]. Furthermore, epithelialization of designed urethral transplants necessitates the creation of a new blood vessel network to sustain feeding and metabolic activity [40].

It is well-known that epithelial cells and smooth muscle cells are embedded in the extracellular matrix (ECM), which is rich in collagen and elastin, in the natural urethra, and retain epithelial and contractile phenotypes [33]. The invention of urethral scaffold transplants that can mimic the anatomy and physiology of native urethral ECM is critical for urethral tissue engineering from a bionics standpoint [47]. Electrospinning is a versatile and widely used method for creating bionic structures to natural urethra with very well hierarchy layouts [15]. Electrospun nanofiber scaffolds have morphological characteristics that are more identical to ECM than other traditional tissue engineering scaffolds [10]. Electrospun nanofibrous scaffolds have also interrelated porous morphologies that mimic the layout of native ECM, permitting them to act as a provisional channel for cell adhesion, mobility, and multiplication for urethral reconstruction [14].

Several synthetic polymers such as poly(L-lactide-co-caprolactone, poly(lactic-co-glycolic acid) [15], poly-lactic acid [1], poly(trimethylene carbonate) [29], and polycaprolactone have been researched for make biomimetic scaffolds for urethral reconstruction with promising results [48]. have prepared a collagen/poly(L-lactide-co-caprolactone) scaffold for urethral reconstruction with dog model. Because of its elastomeric, extensible, nontoxic, and controllable degrading features, nanofibrous poly(L-lactide-co-caprolactone) (PLCL) co-polymer has attracted the attentions of soft tissue-engineered researchers in recent times. In recent [18], have reported that PLLA/gelatine nanofibrous scaffold has the ability to promote the expression of epithelial and smooth muscle cells for urethral reconstruction in New Zealand rabbit model. However, synthetic polymers cannot properly regulate the cell phenotype because of its hydrophobicity and poor cell adherence [11].

As a result, fabricating natural ploymers with nanofibrous synthetic polymers systematically change the interface pharmacology of final scaffolds [16]. Natural polymers such as collagen and gelatin were frequently utilized in the fabrication of various scaffolding materials for urethral reconstruction [24]. They must be allowed to navigate as the extracellular matrix (ECM), allowing cell development, maturation, and multiplication without inducing immune responses [12]. Fibrinogen, a natural polymer has been viewed as a hopeful material for tissue engineering due to its biocompatibility and biodegradability [35]. Based on the background, we have prepared a electrospun fibrinogen/poly(L-lactide-co-caprolactone) copolymer scaffold for urethral reconstruction and the rescue efficacy was assessed using urethral injury model of New Zealand rabbit.

2. Materials & methods

2.1. Materials

PLCL copolymer of (70:30), which contains 70 mol% of L-lactide, was obtained from Daigang Bio-Tech Co. Ltd. Jinan, China. Lyophilized bovine fibrinogen was purchased from Sigma-Aldrich (USA). The solvent 1,1,1,2,2,2-hexafluoro-2-propanol (HFIP) was purchased from Yumei Co. Ltd. Shanghai, China. Other chemicals and media were purchased from Sigma-Aldrich (USA).

2.2. Preparation of fibrinogen-poly(L-lactide-co-caprolactone) (Fib-PLCL) using electrospinning approach

For the electrospinning solutions preparation, a PLCL solution (8% w/v) was prepared by dissolving PLCL in HFIP. Fibrinogen (8% w/v) was dissolved in 9:1 ratio of HFIP and minimal essential medium (100 mg/mL). Then, the 1:1 ratio of fibrinogen/PLCL blended solution was prepared by mixing together and stirring for 6 h. Finally, the electrospinning process was performed using an Electro Spray Deposition Unit (Kato Tech Co., Kyoto, Japan). The blended solution was transferred to a glass syringe that was fitted with a 22G needle and loaded onto an Electro Spray Deposition Unit. The conditions of the electrospinning processes were maintained as mentioned in Ref. [17].

2.3. Characterization

The surface morphology and diameter of the PLCL and Fib-PLCL scaffolds were studied under Stereoscan 360 scanning electron microscope (SEM) (Cambridge, UK). The average fibre sizes were determined by measuring randomized fibres on SEM images with Image J software. The mechanical characteristics of the PLCL and Fib-PLCL scaffolds were analysed using an Instron-5567 instrument (Instron Corp., US). Finally, a contact angle analyzer (Dataphysics, Germany) was used to evaluate the contact angles of the electrospun scaffolds in order to determine their hydrophilic nature.

2.4. Cell adhesion and proliferation of urothelial cells on Fib-PLCL and PLCL scaffolds

For this study, human urothelial cells were obtained from Shanghai Zhongqiao Xinzhou Biotechnology Co., Ltd, China. In the experiment, urothelial cells were grown to 70%—80% confluence in a culture flask and then transferred to a 24-well plate. Then, the prepared PLCL and Fib-PLCL scaffolds were cut into pieces of 1×1 cm and positioned on the bottom of each plate under sterile environment. Finally, the scaffolds were seeded with cell suspension (10^5 cells/mL) and incubated with 1 mL Dulbecco's Modified Eagle's Medium with 10% foetal bovine serum for 48 h. After incubation, the cell grown-scaffolds were subjected to cell count, SEM analysis, and live cell staining.

2.5. Cell count of adhered cells

For counting the number of urothelial cells have attached and grown on the prepared scaffolds, the experimental scaffolds were transferred to fresh 3.5 cm polystyrene dishes and washed with PBS. Subsequently, 500 μL of 0.25% trypsin—0.22% EDTA solution was added to remove the adhered cells from the scaffolds for collecting single-cell suspensions, followed by 2.5 mL of DMEM containing 10% FBS to stop the digestion. The cell suspension was centrifuged and resuspended in 1 mL of $1\times$ PBS. Finally, the individual cells were counted using a cytometer (Countess II FL, Invitrogen).

2.6. SEM analysis and live cell staining

After 48 h incubation, the cell-seeded scaffolds were washed with PBS and immobilized with 2.5% glutaraldehyde for 16 h at 4 °C. Then, the fixed samples were dehydrated using increasing concentrations of ethanol (20, 40, 60, 80, and 100% v/v) and air-dried. Finally, the dried slides were visualized under SEM instrument (Hitachi SU5000; Hitachi High Technologies Corp., Japan). For live cell staining, the cell-seeded scaffolds were washed using the Live/Dead Viability/Cytotoxicity assay kit, as per the manufacture's instruction. After, the scaffolds were kindly washed with PBS and imaged under a fluorescence microscope (Olympus) (Xu et al., 2015).

2.7. Animal and surgical procedures

IACE (Institutional Animal Ethical Committee) of Shanghai Fifth People's Hospital, Fudan University, China, have authorized the animal study (Ref. No: 2021-0214) and performed them in compliance with committee guidelines. A number of 12 healthy male New Zealand white rabbits (4 months old; weight 2.6 ± 0.2 kg) were uniformly assigned to one of four groups (n = 3): autograft (rabbits' autologous urethral tissue), tissue-engineered autologous PLCL and Fib-PLCL scaffolds, and blank control groups. The animals were anesthetized by intraperitoneal injection of sodium pentobarbital (45 mg/kg) [18]. After urethral catheterization, the penile urethra was exposed and mobilised from the underlying corpus spongiosum by a ventral midline skin incision [9]. Then, a 1×2 cm^2 (width $\times$ length) portion of ventral urethral tissue was removed. Subsequently, the damaged urethral regions were rebuilt with the cell-seeded PLCL and Fib-PLCL scaffolds or autografts using interrupted 6-0 polyglactin sutures [18]. There has been no graft transplantation following the severe urethral defect procedure in the blank group. Post surgery, each animal was placed in its own cage with adequate access to food and water. After 4 month post-transplantation, the experimental animals were slaughtered, and excised the urethral samples for histopathological and immuno-histochemical studies.

2.8. Retrograde urethrography

At 4 month post-transplantation, the retrograde urethrography was conducted in all experimental groups to examine the integrity of the regenerated urethra [18]. The rabbits were put obliquely on the examination table after being given general anaesthesia. A 6-F Foley catheter was placed into the urethra until the balloon reached the urethral opening. 2 mL of sterilised distilled water was used to fill the balloon. Diatrizoate meglumine contrast fluid (M861408; purchased from Guangzhou Pharmaceuticals, Guangzhou, China) was gently injected into the catheter before being subjected to a digital X-ray photography perspective system (SIEMENS, Luminos dRF). For urine flow rate measurement, the bladder was drained through the catheter. The bladder was subsequently filled with a rate of 15 mL/min with water. Once the bladder was completely filled with water, the urine flow rate, urination duration, and urination volume were recorded by the digital X-ray photography perspective system.

2.9. Histological assessment

After 4 month post-transplantation, the experimental animals were slaughtered, and excised the urethral samples for histopathological and immunohistochemical studies. The obtained regenerated urethral tissues were frozen in a cold 4% paraformaldehyde solution for 16 h before being washed with distilled water. The samples were dehydrated in a series of alcohol solutions and then embedded in paraffin (Prasath et al., 2021). Finally, 5 μm sections were cut and stained with hematoxylin/eosin (H&E) and Masson's trichrome staining using normal procedures.

2.10. Immunostaining procedure

The immunostaining was performed to confirm the development of cytokeratins (AE1/AE3, 1:250, Thermo Scientific) and the integrity of the actin cytoskeleton (phalloidin-tetramethylrhodamine B isothiocyanate, 1:500, Sigma-Aldrich) in the experiment samples. Immunohistochemistry with the pancytokeratin marker was used to study the development of cytokeratins and urothelial epithelium in urothelial cells as well as after 4 months of *in vivo* follow-up. The samples were mounted with 4% paraformaldehyde and probed overnight with pancytokeratin primary antibody dilutions. The samples were then treated in a combination of secondary antibody (1:800 Alexa-488 donkey, green fluorescence) and phalloidin the next day. Subsequently, the cell nuclei were dyed with DAPI (1: 2000, Sigma-Aldrich) and examined using a fluorescence microscope (Olympus) [29].

3. Results and discussion

3.1. Synthesis and characterization of Fib-PLCL nanofiber scaffold

Electrospinning had already been shown to be a simple and efficient process for producing materials with anisotropic architecture [43]. In the present study, we have prepared a biocompatible fibrinogen−PLCL nanofiber scaffold using electrospinning method for urethral injury treatment. At first, we have investigated the shape of prepared Fib-PLCL nanofiber scaffold and PLCL nanofiber scaffold to demonstrate the physical characteristics of scaffold materials using SEM analysis. The SEM analysis illustrated that the prepared nanofiber of Fib-PLCL is smooth and uniform (Fig. 1a). In comparison, the nanofibres in a pure PLCA scaffold without fibringen exhibit a somewhat rough surface with a little larger fibre diameter and pore size. The mean diameter of the Fib-PLCL fibre is thinner and lighter than the PLCL fibre, and lowered from ~841 nm to ~612 nm (Fig. 1b). The pore size in the Fib-PLCL nanofiber scaffold was shorter than the PLCL nanofiber due to the blending of fibrinogen on the scaffold's surface. The reduced size found in the Fib-PLCL nanofibrous scaffold could help in efficient cell proliferation across surrounding tissues. And, the Fib-PLCL nanofibrous scaffold was exceedingly easy to control and stitch throughout the procedure, substantially resembling native tissues to restore urethral function/plasticity. Then, the mechanical properties of the scaffolds showed that the Fib-PLCL nanofibrous scaffold exhibited lower tensile strength (MPa) (Fig. 1c) compared to PLCL nanofibrous scaffold. In the same way, Fib-PLCL nanofibrous scaffold exhibited higher tensile deformation (Fig. 1d) and suture retention strength compared with PLCL nanofiber scaffold (Fig. 1e). The tensile strength values were notably different, and the fracture toughness of the Fib-PLCL scaffold was substantially larger than those of the PLCL scaffold, indicating its considerable flexibility. In Fig. 1f, the average water contact angles of PLCL scaffold and Fib-PLCL scaffold were observed to the range of 90.51° and 66.94°, respectively. This result suggests that the fibrinogen-coating improved the hydrophilicity of PLCL nanofibers, most likely owing to the influence of hydroxyl and carboxyl groups in the fibrinogen. The Fib-PLCL exhibited better hydrophilicity than PLCL scaffold; hence we believe that it will promote the cell adhesion and proliferation of urothelial cells on their surface.
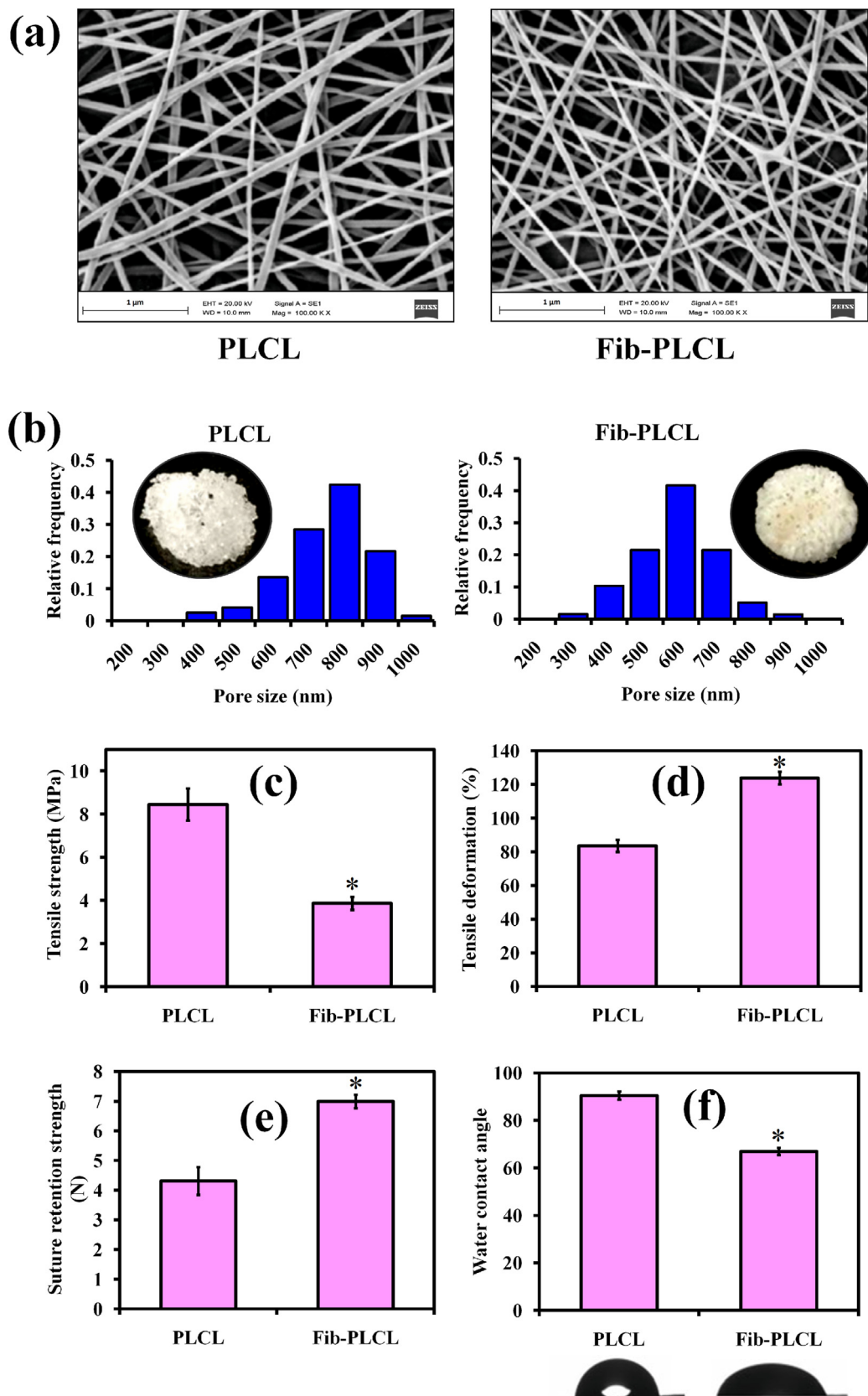
Fig. 1. (a) Structural characterization of the prepared electrospun Fib-PLCL and PLCL nanofiber scaffolds using SEM analysis. (b) Mean pore size of electrospun Fib-PLCL and PLCL nanofiber scaffolds. Inset: Photomicrographs of prepared electrospun Fib-PLCL and PLCL nanofiber scaffolds. Graphs representing the mechanical strength of prepared electrospun Fib-PLCL and PLCL nanofiber scaffolds, including (c) tensile strength, (d) tensile deformation, (e) suture retention strength, and (f) water contact angle. Data are represented as mean ± SD; * indicates $P < 0.05$ compared with PLCL group.

3.2. Fib-PLCL scaffold promotes the cell attachment and viability of urothelial cells

It is well-documented that the nanofibrous matrix ought to be biocompatible as a possible scaffold material for urethral injury treatment and it should allow urothelial cells to cell attachment and their proliferation for urethral reconstruction [49,18]. From a bionic implants standpoint, creating urethral scaffolds competent of duplicating the organization and functioning of the extracellular matrix (ECM) is critical for urethral restoration. Hence, we have examined the capability of the prepared Fib-PLCL nanofibrous scaffold interfaces for cell attachment and proliferation of
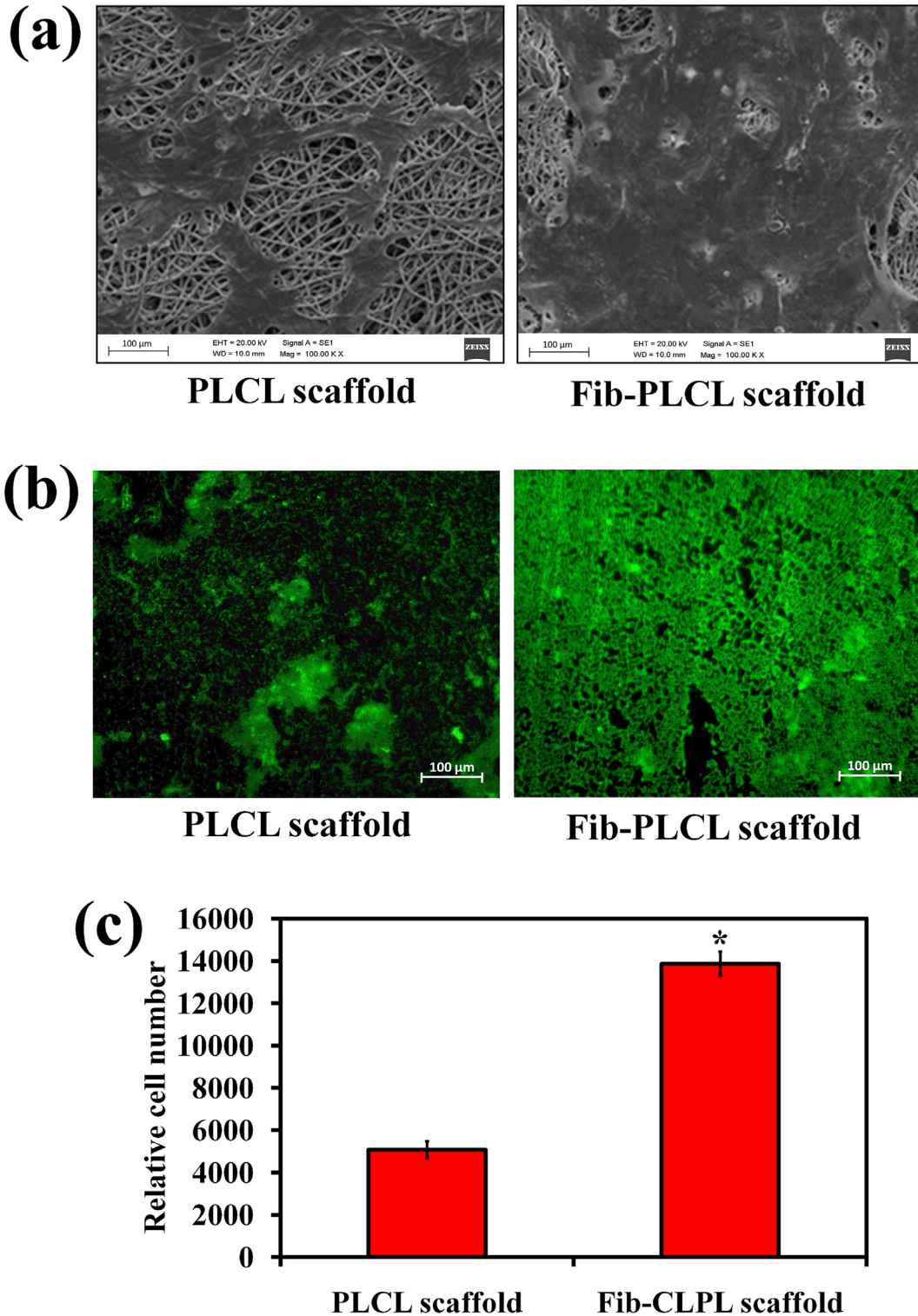

Fig. 2. (a) SEM images of urothelial cell attachment on the Fib-PLCL and PLCL nanofiber scaffolds. (b) Live cell staining of adhered urothelial cells on the surface of the Fib-PLCL and PLCL nanofiber scaffolds. (c) Graph representing the cell count of adhered urothelial cells on the surface of the Fib-PLCL and PLCL nanofiber scaffolds after 48 h. Data are represented as mean ± SD; * indicates $P < 0.05$ compared with PLCL group.

urothelial cells, taking into account the impacts of compositions, wettability, and mechanical characteristics of the fibrous scaffolds on cellular functions. As expected, urothelial cells were attached and grown well on the prepared scaffolds after cell seeding. The SEM analysis illustrated that the Fib-PLCL scaffold appear to promote stronger cell adhesion and growth than PLCL scaffold by developing adherent monolayers with single cells (Fig. 2a). Simultaneously, minimal numbers of cells were migrated and proliferated on the PLCL scaffold. The live cell staining also established that the most of cells were viable on both the PLCL and Fib-PLCL scaffolds (Fig. 2b). The augmented green fluorescence indicating the increased number of cells was grown on the surface of Fib-PLCL scaffold when compared to the PLCA scaffold. Furthermore, the cell population of urothelial cells highly improved in the Fib-PLCL scaffold when compared to the PLCA scaffold after 24 h post-seeding (Fig. 2c), demonstrating that the Fib-PLCL scaffold had no influence on proliferation of urothelial cells. These data suggest that the Fib-PLCL nanofibrous scaffold enhances the cell attachment and proliferation of urothelial cells.

3.3. Fib-PLCL scaffold promotes the cytoskeletal organization in vitro

In the natural urethra, epithelial cells and smooth muscle cells are embedded in the extracellular matrix (ECM), which is rich in collagen, elastin, and cytokeratin, and retain epithelial and contractile phenotypes [32]. Such traits are tightly connected to the expression of ECM-specific characteristics [36]. Hence, immunofluorescence labelling was used in this work to assess the expression of cytokeratins (AE1/AE3, an essential membrane surface protein marker) by cells cultured on the prepared scaffolds [18]. In addition, actin, an ECM protein, was also immunostained with phalloidin to see if these nanofibrous scaffolds could assist urothelial cells to develop anisotropic tissues. In Fig. 3a, the fluorescence microscopic result also revealed that reduced urothelial cells were adhered and grown on the PLCL nanofibrous scaffold. The respective fluorescence intensity is indicating the expression levels of cytokeratin and actin filaments in urothelial cells (Fig. 3b). The result found that the increased expression levels of cytokeratin and
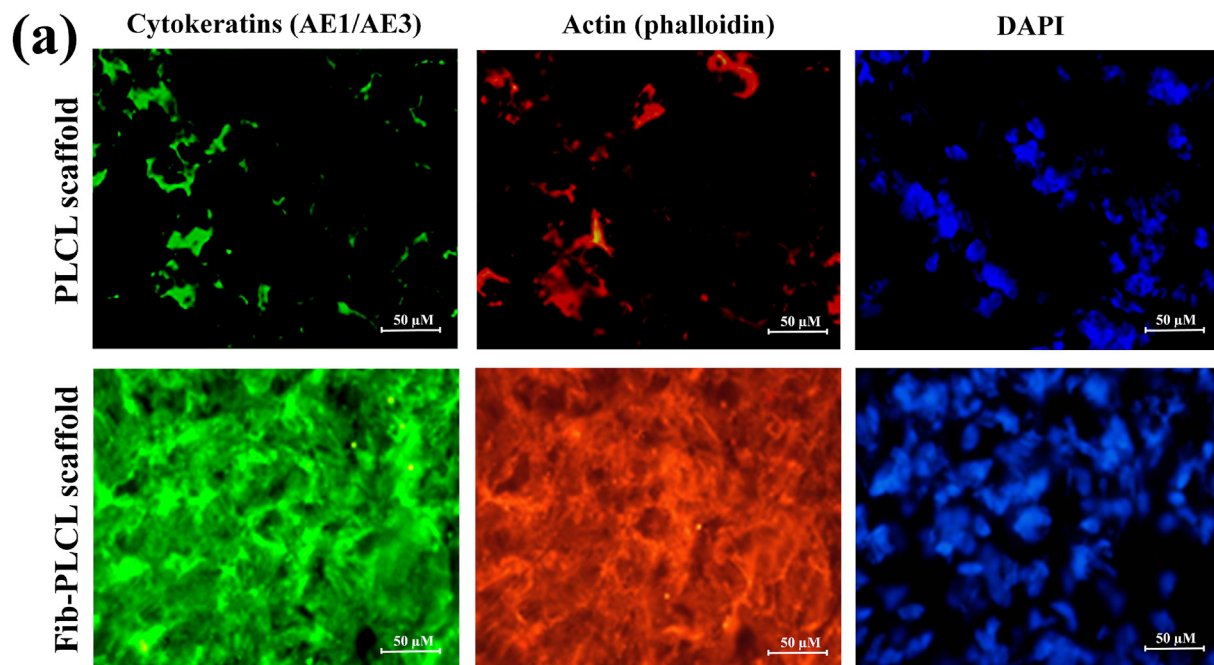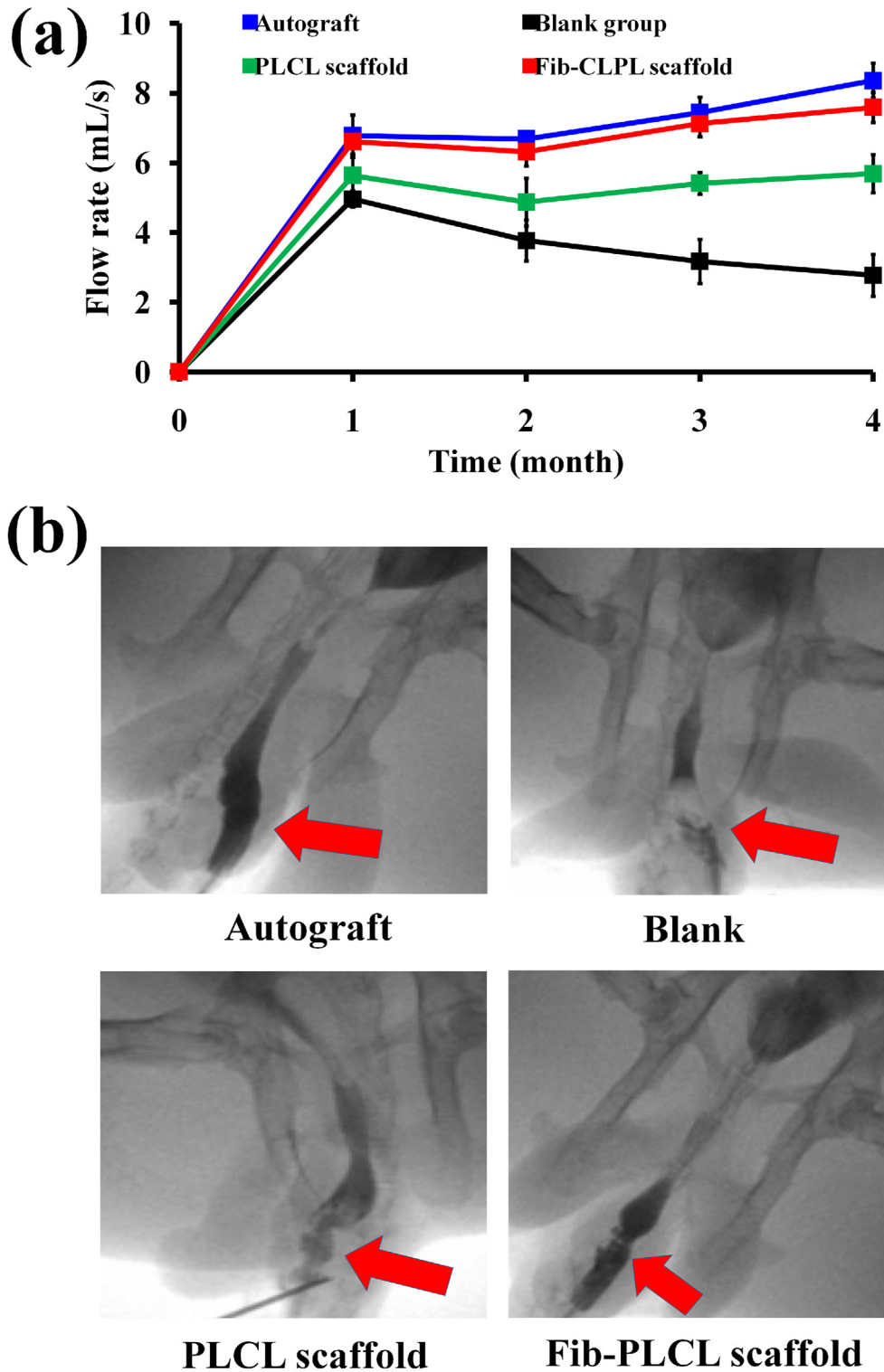

Fig. 3. (a) *In vitro* cell phenotypic expression and extracellular matrix synthesis. Immunofluorescent staining images of cellularized Fib-PLCL and PLCL nanofiber scaffolds stained for cytokeratin (AE1/AE3, green), actin filaments (red), and nuclei (blue) in epithelial cells at 48 h after seeding. (b) Graph representing the relative fluorescence intensity of cytokeratin (AE1/AE3, green) and actin filaments (red) in epithelial cells at 48 h after seeding. Data are represented as mean ± SD; * indicates P < 0.05 compared with PLCL group.

using a rabbit urethral replacement model with three groups: autograft, PLCL, and Fib-PLCL nanofibers. In comparison to the PLCL scaffold, the Fib-PLCL scaffold seemed much more flexible during the surgery and was simpler to stitch and shape into tubular forms around the catheter. The rabbits healed quickly following the surgery. After 2–4 days, the majority of the rabbits resumed regular eating and drinking and urinated on their own. It is known that urination requires a pristine urethral lumen supported with urethral transplants or grafts [33,23]. We assessed the urine flow rate and retrograde urethrography of each rabbit participant at predefined time intervals to examine the post-operative healing effectiveness of the prepared scaffolds [44,13,16]. By a month, all animals in the autograft and Fib-PLCL scaffold groups became capable to pass urine on their own and retained this competence throughout 4 months. The urine average flow rate (AFR) of rabbits in the Fib-PLCL scaffold group (7.5 ± 0.4 mL/s) was nearly similar to the autograft group (8.3 ± 0.5 mL/s) by 4 months (Fig. 4a). In contrary, all animals in the PLCL scaffold group suffered their frequent urination (5.6 ± 0.5 mL/s), and all animals in the blank control groups had urethral injuries (2.7 ± 0.6 mL/s).

Retrograde urethrography images illustrated that the animals in the autograft and Fib-PLCL scaffold groups exhibited urethral lumen functional capacity 4 months after transplantation (Fig. 4b). Both the autograft and Fib-PLCL scaffold groups were able to successfully excrete the contrast agent by their neourethras [18]. In addition, the urethral diameter in the Fib-PLCL scaffold group (2.7 ± 0.3 mm) is also similar to the autograft group (2.9 ± 0.2 mm). The urethral diameter in the PLCL scaffold group (2.1 ± 0.2 mm) was lesser than that of the Fib-PLCL scaffold group. Importantly, there was no regenerated neourethra in the blank group because there

was no scaffold insertion; hence, no contrast agent was seen. Due to the efficient urethral regeneration *in vivo*, the present study suggests that the prepared Fib-PLCL nanofibrous scaffold can be used as a potent scaffolding material for urethral injury treatment.

3.5. Fib-PLCL scaffold improves the epithelial tissue regeneration in vivo

The urethral smooth muscle's major role is to perpetuate urination via contraction, and the urethral epithelium's primary function would be to assure that urine flowing properly through the urethra [46]. The epithelial tissue layer might act as a barrier to urethral infiltration and minimise physiological friction upon implantation, hence epithelial development is vital for making urethral reconstruction [40,4]. A strong epithelial layer can prevent urethral atresia in the regenerated urethra [27]. In order to confirm the urethral epithelialization efficacy of Fib-PLCL scaffold graft, H&E staining, and Masson's trichrome staining were performed after 4 months. In Figs. 5a & S1, the black colour arrow represents that the urethral skeletal muscle cells grew consistently in the Fib-PLCL scaffold group, and the lumen of the nascent urethral tissue was enclosed with urethral epithelial cell layers, forming full urinary tract epithelial tissue, which similar to autograft group. Simultaneously, the red colour arrow illustrates that a considerable urethral tissue development is not shown in the PLCL scaffold group, compared to the Fib-PLCL scaffold group. Furthermore, the Masson's trichrome staining results showed that the regenerated urethral smooth muscles (red colour) and collagen layers (blue colour) are immediately evident and uniformly distributed in the Fib-PLCL scaffold graft group (Fig. 5b), as like autograft group.
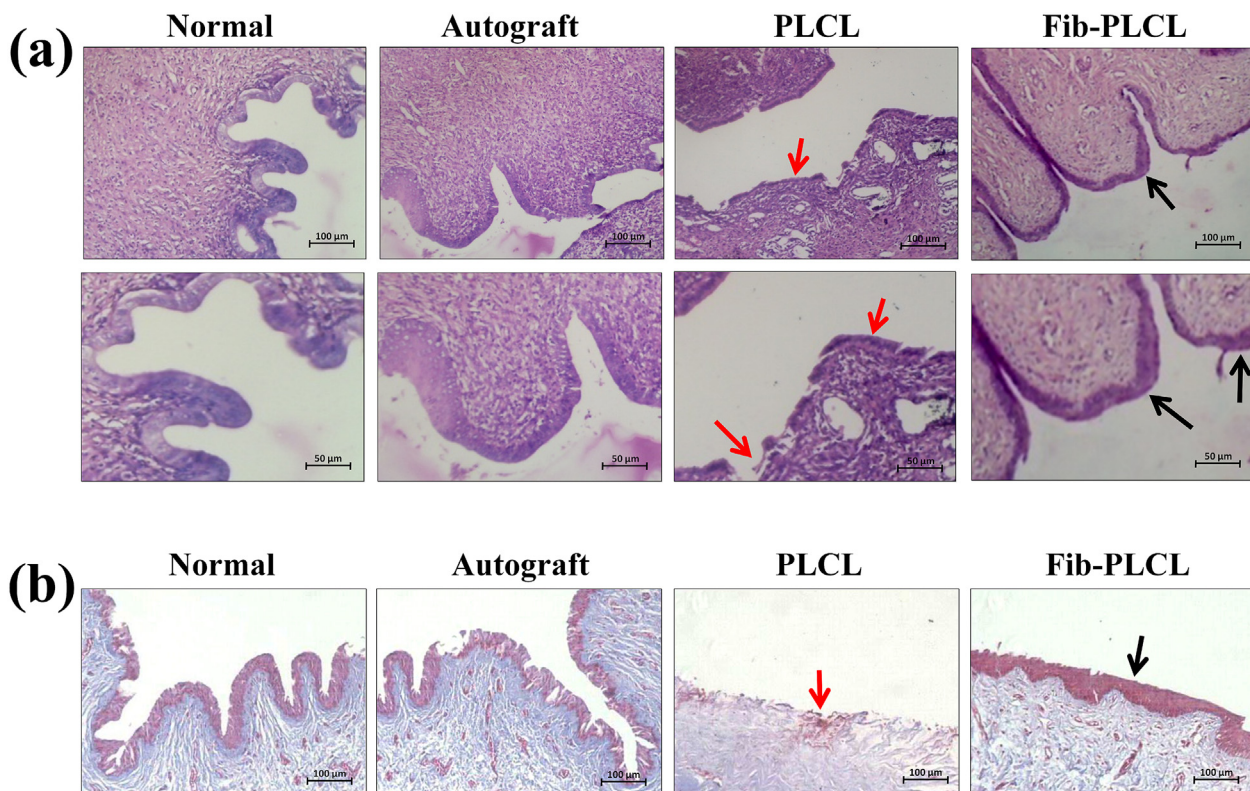
Fig. 5. Histological analysis of urethral epithelial layer reconstruction in the Fib-PLCL and PLCL scaffolds implanted rabbits. (a) H&E staining micrographs and (b) Masson's trichrome micrographs of a cross-section of urethral epithelial layer of each graft scaffolds implanted rabbits in the urethral defective site after 4 months. The black colour arrow designates that the urethral skeletal muscle cells showed uniform growth with layers of urethral epithelial cells, generating a whole urinary tract epithelium in the Fib-PLCL scaffold, similar to the autograft group. The red colour arrow indicates that a significant amount of urethral tissue growth is not seen in the PLCL scaffold group, compared to the Fib-PLCL scaffold group.

Herein, the black colour arrow indicated that the rate of urethral epithelialisation in the Fib-PLCL scaffold group is higher. In the PLCL group, the red colour arrow indicates that urethral epithelium in the lumens was little weak compared to Fib-PLCL group. Both H&E and Masson's trichrome staining findings demonstrated that the repaired urethras in the Fib-PLCL graft group had generated multilayered urothelium layers that resembled normal urothelium. Since the regenerated urothelial cells could fill the Fib-PLCL scaffold's surface, the mechanical strength of the reconstructed urethral smooth muscle tissues was satisfactory, resulting in urethral epithelialization and reconstruction [1].

3.6. Fib-PLCL scaffold promotes the cytoskeletal organization in vivo

In order to identify the histopathological constituents of the regenerated urethra such as cytokeratins (AE1/AE3) and actin cytoskeleton organization (phalloidin) in regenerated urethra, immunofluorescent staining was performed [42,16]. The microscopic images clearly illustrated that the strong emission of green and red fluorescence of cytoskeleton markers (AE1/AE3 and phalloidin) indicating the development of cytokeratins and actin filaments in the reconstructed urethra of Fib-PLCL scaffold group (Fig. 6a), demonstrated the formation of de novo urothelium. The yellow colour arrow indicates that the cytokeratins and actin

filaments were strongly expressed in the regenerated urothelium of Fib-PLCL scaffold group (Fig. 6b). However, the cytokeratin expression was relatively low, and the actin filaments appeared to congregate lightly on the border of cell cytoskeleton in the PLCL scaffold, as indicated by red colour arrow. This result was correlated with the *in vitro* immunofluorescence staining results (Fig. 3). The epithelium in the Fib-PLCL group was composed of 9—12 sheets of layered epithelial cells and surrounded the whole portion of the regenerated urethra. The epithelial cells were grouped in an ordered fashion, had normal morphology, and resembled the urothelium of a normal urethra. The epithelium in the PLCL group was composed of 3—5 layers of layered epithelial cells and seemed to be smaller than normal urothelium. The epithelial cells have been organised weakly in the PLCL group and was not completely covered by an epithelial tissue layer in the topmost layer. The average depth of the epithelial layer in the Fib-PLCL group was 117.3 ± 3.2 μm, which was nearly similar to autograft group (120.1 ± 2.7 μm) and much larger than the PLCL group (9.6 ± 2.2 μm) (Fig. 6c). The repaired urethra attained a persistent squamous epithelial pattern and contractile morphology *in vivo* due to the continuous stratified nanofibers structure of the prepared scaffold grafts, which may sustain urothelial cells-seeded matrices in a 3D space [18]. Similarly, hyaluronic acid-silk fibroin scaffold enhanced the urethral epithelialisation with improved expression of cytokeratins and actin filaments in the reconstructed
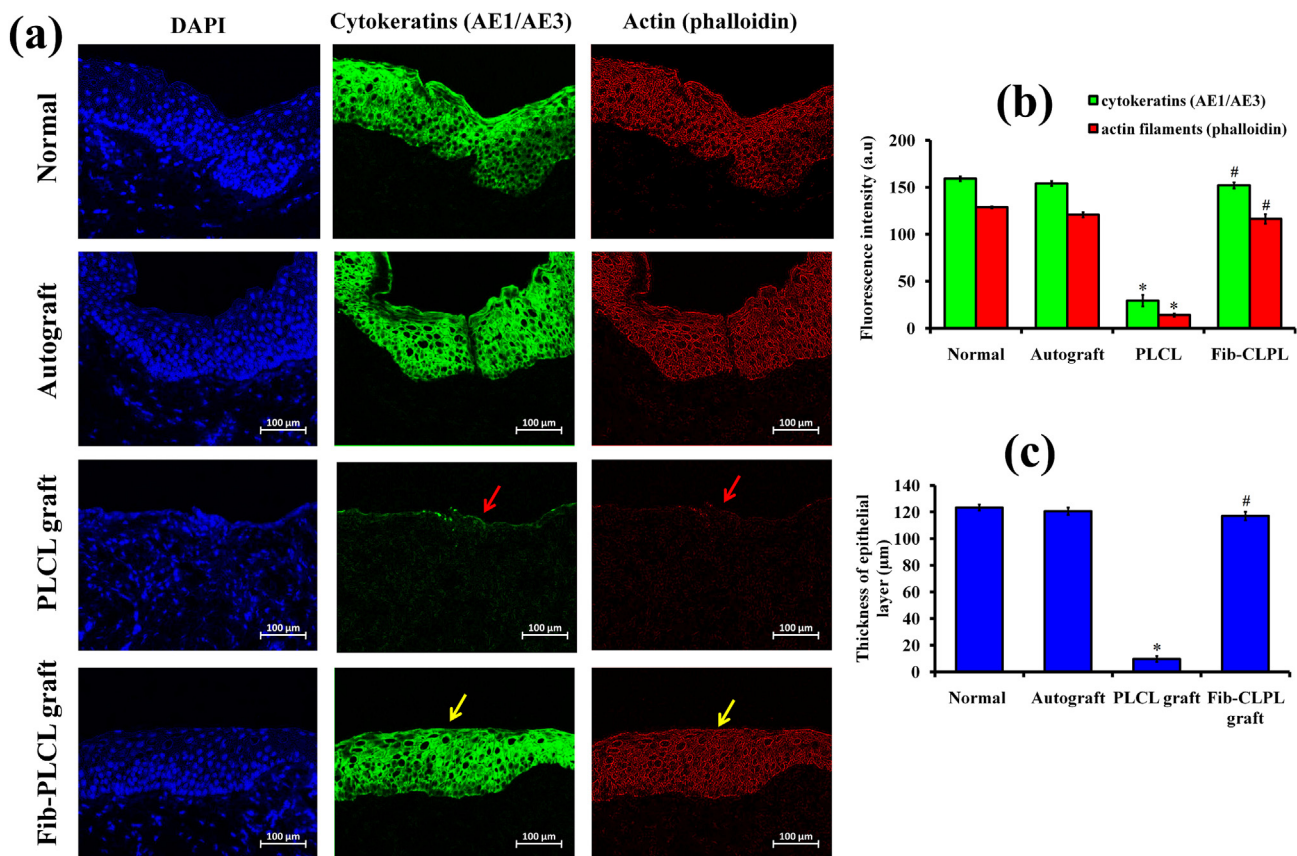
Fig. 6. Fib-PLCL scaffold promoteed the cytoskeletal organization *in vivo*. (a) Immunofluorescent staining images of cellularized Fib-PLCL and PLCL nanofiber scaffolds stained for cytokeratin (AE1/AE3, green), actin filaments (red), and nuclei (blue) in a cross-section of the mid-section of each graft scaffolds implanted in the urethral defective site. The cytokeratins and actin filaments were significantly expressed in the regenerated urothelium of the Fib-PLCL scaffold group, as shown by the yellow colour arrow. On the other hand, the cytokeratin expression in the PLCL scaffold was somewhat low, and the actin filaments seemed to aggregate lightly on the edge of the cell cytoskeleton, as represented by the red arrow. (b) Graph representing the relative fluorescence intensity of cytokeratin (AE1/AE3, green) and actin filaments (red) in epithelial cells at 4 months after surgery. Data are represented as mean ± SD; * indicates P < 0.05 compared with PLCL group. (c) Graph representing the relative thickness of epithelial layer in a cross-section of the mid-section of each graft scaffolds implanted in the urethral defective site. Data are represented as mean ± SD; * indicates P < 0.05 compared with autograft group and # indicates P < 0.05 compared Fib-PLCL group with PLCL graft group.
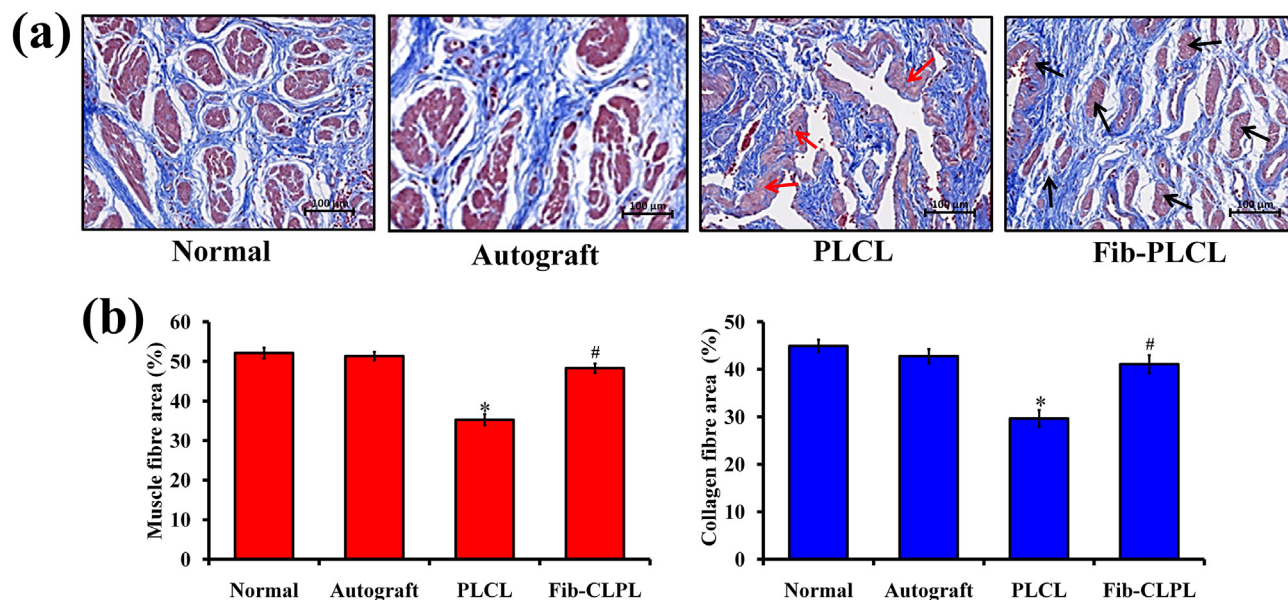
Fig. 7. Histological analysis of smooth muscle cell development in the Fib-PLCL and PLCL scaffolds implanted rabbits. The Fib-PLCL scaffold graft group's regenerated urethra was clearly characterised by a black colour arrow, which showed large number of freshly regenerated smooth muscle bundles; in contrast, the red colour arrow revealed a lower ratio of newly regenerated smooth muscle bundles in the PLCL scaffold group.

urethra. The outcome of this study revealed that the prepared Fib-PLCL scaffold grafts regenerated a substantial number of cytokeratins (AE1/AE3) and actin cytoskeleton filaments in the regenerated urethra (see Fig. 7).

3.7. Fib-PLCL scaffold enhanced the reconstruction of smooth muscle bundle and collagen fibres

Smooth muscles and collagen fibres are important components in the reconstruction of urethra [49,25]. Hence, Masson's trichrome staining was used to investigate the development of the smooth muscle bundle and collagen nanofibers in the reconstructed urethra [46]. At 4 months after transplantation, the anatomy of the newly regenerated smooth muscle bundles (red) in the rejuvenated urethra of the Fib-PLCL scaffold graft group was closer to the native urethra (Fig. 6a). The black colour arrow clearly indicated the newly regenerated smooth muscle bundles in the rejuvenated urethra of the Fib-PLCL scaffold graft group. At the same time, the ratio of regenerated smooth muscle bundles in the PLCL scaffold group was lesser, as marked by red colour arrow. The area percentage of smooth muscle in the Fib-PLCL group was 48.31%, which was greater than the PLCL group (35.26%) and equivalent to the normal urethra (52.12%), as shown in Fig. 6b. Similarly, the area percentage of collagen fibres in the Fib-PLCL group was higher than the PLCL group, which comparable to the normal urethra. These results recommended that the prepared urethral graft of Fib-PLCL scaffold can promote the regeneration of smooth muscle bundle and collagen fibres at the wounded site, resulting in urethral reconstruction.

It is known that nanofibrous fibrinogen has been shown to offer a good favourable environment for the proliferation and differentiation of human bladder smooth muscle cells, as well as the ability to be modified by seeded cells for urethral reconstruction [20,22,21]. As expected, the presence of fibrinogen in the prepared Fib-PLCL scaffold is mainly contributing to promote the urethral tissue development. Our *in vitro* and *in vivo* results found that the Fib-PLCL scaffold has the ability to improve the epithelial tissue regeneration with enhanced the cytoskeletal organization as well

as reconstruction of smooth muscle bundle and collagen fibres in regenerated urethra. Therefore, the present study suggests the prepared Fib-PLCL scaffold as a potent graft material for urethral reconstruction.

4. Conclusion

In conclusion, we successfully fabricated the fibrinogen-functionalized PLCL tubular nanofibrous scaffolds using electrospinning method. As a result, the resultant hydrophilic and biocompatible Fib-PLCL nanofibrous scaffolds exhibit efficient mechanical qualities similar to the native urethra for cell attachment and proliferation of urethelial cells. Human epithelial cells grown on Fib-PLCL scaffolds developed spindle-like and triangular-oriented architectures, probably as a result of the synergistic impact of the micro-porous framework and pharmacological regulation. Notably, when compared to cells on the PLLA scaffold, the Fib-PLCL scaffold was found to encourage the cell propagation of epithelial cells and to retain the cells in their relevant cytoskeletal and epithelial phenotypes, as indicated by increased the expression level of cytokeratin (AE1/AE3). Furthermore, we demonstrated that the distinctive structural protein of actin filaments was properly formed on the Fib-PLCL nanofibrous scaffold. Animal studies have also revealed that designed cellularized Fib-PLCL scaffold graft might very well induce luminal epithelialization, urethral smooth muscle cell remodelling, and capillary development all at the same time. The robustness of these findings shows that fibrinogen-functionalized PLCL nanofibrous scaffolds have a synergistic action on epithelial and smooth muscle cell regeneration *in vitro* and *in vivo*. Based on the results, the present study suggests that the cellularized fibrinogen–PLCL scaffold is more suitable for urethral reconstruction in urethral injury treatment.

Data availability statement

All the data presented in the study are included in the article/Supplementary material.

Authors' contribution

WJ: Conceptualization performed the experiments, data analysis, and writing-original draft. WY: formal analysis, data analysis. YW: formal analysis, data analysis. YZ: formal analysis, data analysis. YW: formal analysis, data analysis. HH: formal analysis, data analysis. GS: Conceptualization, Supervision, data analysis, and reviewing-original draft. All authors contributed to the article and approved the submitted version.

Declaration of competing interest

All the authors declare that the research was conducted in the absence of any commercial or financial relationships that could be construed as a potential conflict of interest.

Acknowledgement

Appendix A. Supplementary data

Supplementary data to this article can be found online at https://doi.org/10.1016/j.reth.2022.12.004.

References

[1] Abbas TO, Yalcin HC, Pennisi CP. From acellular matrices to smart polymers: degradable scaffolds that are transforming the shape of urethral tissue engineering. Int J Mol Sci 2019 Jan;20(7):1763.

[2] Adamowicz J, Kuffel B, Van Breda SV, Pokrwczynska M, Drewa T. Reconstructive urology and tissue engineering: converging developmental paths. J Tissue Eng Regen Med 2019 Mar;13(3):522−33.

[3] Algarrahi K, Affas S, Sack BS, Yang X, Costa K, Seager C, et al. Repair of injured urethras with silk fibroin scaffolds in a rabbit model of onlay urethroplasty. J Surg Res 2018 Sep 1;229:192−9.

[4] Badylak SF. Xenogeneic extracellular matrix as a scaffold for tissue reconstruction. Transpl Immunol 2004 Apr 1;12(3−4):367−77.

[5] Barratt RC, Bernard J, Mundy AR, Greenwell TJ. Pelvic fracture urethral injury in males—mechanisms of injury, management options and outcomes. Transl Androl Urol 2018 Mar;7(Suppl. 1):S29.

[6] Battaloglu E, Figuero M, Moran C, Lecky F, Porter K. Urethral injury in major trauma. Injury 2019 May 1;50(5):1053−7.

[7] Casarin M, Morlacco A, Dal Moro F. Tissue engineering and regenerative medicine in pediatric urology: urethral and urinary bladder reconstruction. Int J Mol Sci 2022 Jan;23(12):6360.

[8] Chen J, Liao C, Zhao H, Zhao W, Chen Z, Wang Y. Application of tissue engineering urethral stent and its preparation technology in urethral reconstruction. Chin J Tissue Eng Res 2021 Aug 8;25(22):3591.

[9] Chung YG, Tu D, Franck D, Gil ES, Algarrahi K, Adam RM, et al. Acellular bilayer silk fibroin scaffolds support tissue regeneration in a rabbit model of onlay urethroplasty. PLoS One 2014 Mar 14;9(3):e91592.

[10] Culenova M, Bakos D, Ziaran S, Bodnarova S, Varga I, Danisovic L. Bioengineered scaffolds as substitutes for grafts for urethra reconstruction. Materials 2019 Jan;12(20):3449.

[11] de Kemp V, de Graaf P, Fledderus JO, Ruud Bosch JL, de Kort LM. Tissue engineering for human urethral reconstruction: systematic review of recent literature. PLoS One 2015 Feb 17;10(2):e0118653.

[12] Fan S, Chen K, Yuan W, Zhang D, Yang S, Lan P, et al. Biomaterial-based scaffolds as antibacterial suture materials. ACS Biomater Sci Eng 2020 Mar 31;6(5):3154−61.

[13] Horiguchi A, Ojima K, Shinchi M, Kushibiki T, Mayumi Y, Miyai K, et al. Successful engraftment of epithelial cells derived from autologous rabbit buccal mucosal tissue, encapsulated in a polymer scaffold in a rabbit model of a urethral stricture, transplanted using the transurethral approach. Regen Ther 2021 Dec 1;18:127−32.

[14] Hu J, Ai B, Zhu S, Wang Z, Xia H, Jia W. Electrospun PLGA and PLGA/gelatin scaffolds for tubularized urethral replacement: studies in vitro and in vivo. J Biomater Appl 2022 Jan;36(6):956−64.

[15] Huang L, Wang X, Zhang Y, Cheng Z, Xue F, Guo Y, et al. Electrospun Mg/poly (lactic-co-glycolic acid) composite scaffold for urethral reconstruction. J Mater Sci 2020 Sep;55(27):13216−31.

[16] Jia W, Tang H, Wu J, Hou X, Chen B, Chen W, et al. Urethral tissue regeneration using collagen scaffold modified with collagen binding VEGF in a beagle model. Biomaterials 2015 Nov 1;69:45−55.

[17] Li S, Su L, Li X, Yang L, Yang M, Zong H, et al. Reconstruction of abdominal wall with scaffolds of electrospun poly (L-lactide-co caprolactone) and porcine fibrinogen: an experimental study in the canine. Mater Sci Eng C 2020 May 1;110:110644.

[18] Liu G, Fu M, Li F, Fu W, Zhao Z, Xia H, et al. Tissue-engineered PLLA/gelatine nanofibrous scaffold promoting the phenotypic expression of epithelial and smooth muscle cells for urethral reconstruction. Mater Sci Eng C 2020 Jun 1;111:110810.

[19] Marzi J, Brauchle EM, Schenke-Layland K, Rolle MW. Non-invasive functional molecular phenotyping of human smooth muscle cells utilized in cardiovascular tissue engineering. Acta Biomater 2019 Apr 15;89:193−205.

[20] McManus M, Boland E, Sell S, Bowen W, Koo H, Simpson D, et al. Electrospun nanofibre fibrinogen for urinary tract tissue reconstruction. Biomed Mater 2007 Nov 2;2(4):257.

[21] McManus MC, Boland ED, Bowlin GL, Simpson DG, Espy PG, Koo HP. 1728: electrospun fibrinogen nanofiber matrix for urologic tissue engineering. J Urol 2004 Apr;171(4S):457.

[22] McManus MC, Sell SA, Bowen WC, Koo HP, Simpson DG, Bowlin GL. Electrospun fibrinogen-polydioxanone composite matrix: potential for in situ urologic tissue engineering. J Eng Fibers Fabr 2008 Jun;3(2):155892500800300204.

[23] Niu Y, Liu G, Chen C, Fu M, Fu W, Zhao Z, et al. Urethral reconstruction using an amphiphilic tissue-engineered autologous polyurethane nanofiber scaffold with rapid vascularization function. Biomater Sci 2020;8(8):2164−74.

[24] Orabi H, Martins FE. Tissue engineering in urethral reconstruction. In: Textbook of male genitourethral reconstruction. Cham: Springer; 2020. p. 437−45.

[25] Pinnagoda K, Larsson HM, Vythilingam G, Vardar E, Engelhardt EM, Thambidorai RC, et al. Engineered acellular collagen scaffold for endogenous cell guidance, a novel approach in urethral regeneration. Acta Biomater 2016 Oct 1;43:208−17.

[26] Podesta M, Podesta Jr M. Traumatic posterior urethral strictures in children and adolescents. Front Pediatr 2019 Feb 19;7:24.

[27] Rashidbenam Z, Jasman MH, Hafez P, Tan GH, Goh EH, Fam XI, et al. Overview of urethral reconstruction by tissue engineering: current strategies, clinical status and future direction. Tissue Eng Regen Med 2019 Aug;16(4):365−84.

[28] Saad S, Osman NI, Chapple CR. Tissue engineering: recent advances and review of clinical outcome for urethral strictures. Curr Opin Urol 2021 Sep 1;31(5):498−503.

[29] Sartoneva R, Kuismanen K, Juntunen M, Karjalainen S, Hannula M, Kyllönen L, et al. Porous poly-l-lactide-co-ϵ-caprolactone scaffold: a novel biomaterial for vaginal tissue engineering. R Soc Open Sci 2018 Aug 15;5(8):180811.

[30] Scarberry K, Bonomo J, Gómez RG. Delayed posterior urethroplasty following pelvic fracture urethral injury: do we have to wait 3 months? Urology 2018 Jun 1;116:193−7.

[32] Sharma AK, Cheng EY. Growth factor and small molecule influence on urological tissue regeneration utilizing cell seeded scaffolds. Adv Drug Deliv Rev 2015 Mar 1;82:86−92.

[33] Sharma S, Basu B. Biomaterials assisted reconstructive urology: the pursuit of an implantable bioengineered neo-urinary bladder. Biomaterials 2022 Feb 1;281:121331.

[35] Stapelfeldt K, Stamboroski S, Mednikova P, Brüggemann D. Fabrication of 3D-nanofibrous fibrinogen scaffolds using salt-induced self assembly. Biofabrication 2019 Mar 1;11(2):025010.

[36] Sun TT. Altered phenotype of cultured urothelial and other stratified epithelial cells: implications for wound healing. Am J Physiol Ren Physiol 2006 Jul;291(1):F9−21.

[37] Sylla P, Knol JJ, D'Andrea AP, Perez RO, Atallah SB, Penna M, et al. Urethral injury and other urologic injuries during transanal total mesorectal excision: an international collaborative study. Ann Surg 2021 Aug 12;274(2):e115−25.

[38] Tae BS, Yoon YE, Na W, Oh KJ, Park SY, Park JY, et al. Epidemiologic study of bladder and urethral injury in Korea: a nationwide population-based study. Investig Clin Urol 2022 Jan;63(1):92.

[39] Tian B, Song L, Liang T, Li Z, Ye X, Fu Q, et al. Repair of urethral defects by an adipose mesenchymal stem cell-porous silk fibroin material. Mol Med Rep 2018 Jul 1;18(1):209−15.

[40] Wan X, Xie MK, Xu H, Wei ZW, Yao HJ, Wang Z, et al. Hypoxia-preconditioned adipose-derived stem cells combined with scaffold promote urethral reconstruction by upregulation of angiogenesis and glycolysis. Stem Cell Res Ther 2020 Dec;11(1):1−6.

[41] Wang C, Chen C, Guo M, Li B, Han F, Chen W. Stretchable collagen-coated polyurethane-urea hydrogel seeded with bladder smooth muscle cells for urethral defect repair in a rabbit model. J Mater Sci Mater Med 2019 Dec;30(12):1−9.

[42] Wang F, Liu T, Yang L, Zhang G, Liu H, Yi X, et al. Urethral reconstruction with tissue-engineered human amniotic scaffold in rabbit urethral injury models. Med Sci Mon Int Med J Exp Clin Res 2014;20:2430.

[43] Wang Y, Cui W, Zhao X, Wen S, Sun Y, Han J, et al. Bone remodeling-inspired dual delivery electrospun nanofibers for promoting bone regeneration. Nanoscale 2019;11(1):60−71.

[44] Wang Z, Li Q, Wang P, Yang M. Biodegradable drug-eluting urethral stent in limiting urethral stricture formation after urethral injury: an experimental study in rabbit. J Bioact Compat Polym 2020 Jul;35(4−5):378−88.

[46] Wu S, Liu Y, Bharadwaj S, Atala A, Zhang Y. Human urine-derived stem cells seeded in a modified 3D porous small intestinal submucosa scaffold for urethral tissue engineering. Biomaterials 2011 Feb 1;32(5):1317–26.

[47] Xing H, Lee H, Luo L, Kyriakides TR. Extracellular matrix-derived biomaterials in engineering cell function. Biotechnol Adv 2020 Sep 1;42:107421.

[48] Zhang K, Fang X, Zhu J, Yang R, Wang Y, Zhao W, et al. Effective reconstruction of functional urethra promoted with ICG-001 delivery using core-shell collagen/poly (Llactide-co-caprolactone)[P (LLA-CL)] nanoyarn-based scaffold: a study in dog model. Front Bioeng Biotechnol 2020:774.

[49] Zhang K, Guo X, Zhao W, Niu G, Mo X, Fu Q. Application of Wnt pathway inhibitor delivering scaffold for inhibiting fibrosis in urethra strictures: in vitro and in vivo study. Int J Mol Sci 2015 Nov;16(11):27659–76.

[50] Zhang Z, Fang L, Chen D, Li W, Peng N, Thakker PU, et al. A modified endoscopic primary realignment of severe bulbar urethral injury. J Endourol 2021 Mar 1;35(3):335–41.

[51] Zou Q, Fu Q. Tissue engineering for urinary tract reconstruction and repair: progress and prospect in China. Asian J Urol 2018 Apr 1;5(2):57–68.